Rake-Based Cellular Radar Receiver Design for Moving Target Detection in Multipath Channel

Yeejung Kim, Myungdeuk Jeong, and Youngnam Han

In this paper, we design a rake-based cellular radar receiver (CRR) scheme to detect a moving target located in a multipath environment. The modules of Doppler filter banks, threshold level test, and target detection module are newly introduced into the conventional rake receiver so that it can function as a radar system. The proposed CRR tests the Doppler-shift frequency and signal-to-noise ratio of the received signal against predefined threshold levels to determine detection and then calculates target velocities and ranges. The system performance is evaluated in terms of detection probability and the maximum detection range under a Nakagami-n channel that reflects the multipath environment.

Keywords: Cellular radar, bistatic, rake, multipath.

I. Introduction

Recently, cellular radar has received much attention in studies on next-generation radar systems. Cellular radar refers to mobile network–based multi-static radar that use signals radiating from the base station (BS) of a commercial wireless communication system [1]–[5]. One of the unique characteristics of the system is a bistatic radar geometry that consists of a transmitter, target, and receiver. Under this geometry, the bistatic radar cross section (RCS) is sometimes higher than the mono-static RCS depending on the shape of the target. The system provides some benefits — namely, mobility, concealment, and cost saving. A small, lightweight receiver is potentially undetectable to an enemy, so covert operation is possible. In addition, production and maintenance costs can be reduced by using a third party's transmitter.

CELLDAR, which was jointly developed by Roke Manor Research Limited and BAE Systems, both of whom are based in the UK, seems to be the first cellular radar system in this field [2]. The system operates on the basis of the Global System for Mobile Communications (GSM) and hires several modified GSM receivers equipped with two Yagi antennas that receive echo and reference signals. For a code division multiple access (CDMA) network–based system, a signal processing scheme is developed to detect moving targets [4]–[5]. In the researches, the systems employ two directional antennas to receive a target echo and a reference signal. With the reference signal via a direct path, time synchronization with a third party's transmitter is achieved. Then a receiver periodically captures arbitrary signal streams for a certain period of time, and then executes cross-correlation processes for Doppler-shift frequency (DSF) and time delay. Once the processing is complete, the target's velocity and range can be obtained.

The cellular radar system might be colocated with a BS that is installed in urban or suburban areas. In this environment, a radio channel becomes a non-line-of-sight (NLOS) element with multipath components. Since this channel condition acts as a serious obstacle to receiving target echo signals, the detection performance will significantly degrade. Therefore, a receiving technique with superior detection performance and robustness to inferior channel conditions is necessary. For this purpose, we introduce a rake receiver used in commercial CDMA systems in the design of a cellular radar receiver (CRR) to overcome the above problem.

In this paper, we propose a novel receiver scheme for a CRR to detect a moving target in a multipath environment. A Doppler filter bank (DFB) module, a threshold level test (TLT) module, and a target detection (TD) module are newly inserted into the conventional rake receiver to function as a radar system. Using both a DFB and a TLT, the receiver sequentially tests the DSF and signal-to-noise ratio (SNR) of the received signal (namely, radar measurements) against the predefined threshold level to determine target detection. Such two-step threshold testing is suggested for adaptive detection under the region of a forward scattering fence (FSF) where DSF is invalid, while SNR is valid due to bistatic geometry. At last, the velocity and range of a detected target are computed in the TD module. The target location can be obtained by using a bistatic time of arrival (TOA) method, but this is beyond the scope of this paper. Finally, the system performance is evaluated in terms of detection probability and the maximum detection range under a Nakagami-n channel model that reflects the multipath environment.

Section II provides system model considerations. The detection procedures of the CRR are described in Section III. The system performance is evaluated in Section IV, and the effectiveness of this study is summarized in Section V.

II. System Model

1. System Considerations

Figure 1 shows the system modeling of the proposed cellular radar. The following are some of the prerequisite system considerations required in the design of a CRR based on a CDMA network:

▪ Among the various physical down-link channels provided by the CDMA BS, we use the pilot channel as the radar signal because its power and bandwidth are constant during the entire transmission time [6]. These characteristics ensure that the system maintains a stable system performance in terms of range information.

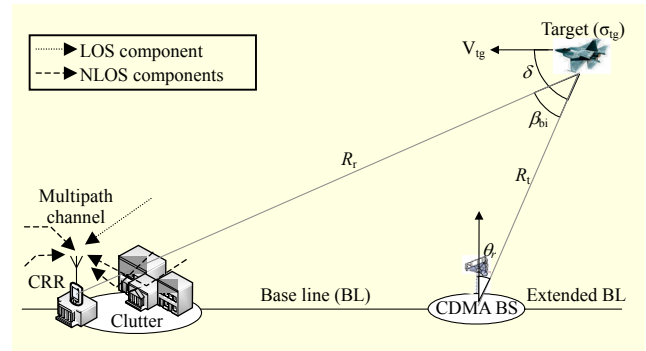▪ The BS transmits a pilot signal with a unique pseudo-

Fig. 1. Cellular radar system model, where R_t (R_r) is the range from a transmitter (receiver) to a target and θ_r is the angle at the receiver to a target.

noise (PN) sequence and excellent auto-correlation, so a rake receiver can extract the desired pilot signal among the signals from various BSs. In addition, a receiver can achieve a time synchronization with high synchronization probability in a multipath fading channel.

▪ We can adjust the parameters, such as the number of fingers and the finger interval of a rake receiver, according to the requirements of the system performance. If you want to increase the range resolution, then employ a rake with densely arranged fingers, which reduces the time-difference interval between the fingers.

▪ A single target's location can be obtained by the algorithm of a bistatic TOA that computes a point in multidimensional space using the range values from multiple CRRs [7]. For multiple targets, conventional tracking algorithms can be applied in the post-processing stage.

▪ We assume a channel without inter-cell interference from neighbors or a remote BS.

▪ A commercial BS normally illuminates its signal toward the ground. However, for this application the signal has to reach a target in the air, so a BS with an isotropic antenna is adopted.

▪ The velocity of a target aircraft is much greater than that of any ground target; thus, we can discriminate the aircraft target with the criterion of DSF.

2. Signal and Channel Model

The CRR is colocated with a CDMA BS and operated in a multipath channel environment, as shown in Fig. 1. Target echo signals with surrounding clutters are fed into the antenna of the CRR. We model the signal and channel as follows.

Transmitter. Equation (1) is the transmitted signal model of the BS [8].

$$s_k(t) = Ad_k(t)c_k(t)\cos(\omega_c t). \tag{1}$$

In (1), k identifies a certain user or channel, the amplitude of

the signal is denoted by A, and the carrier frequency in radian/sec is denoted by ω_c. The bits sequence of the pilot signal and the PN code for the channelization are denoted by $d_k(t)$ and $c_k(t)$, respectively.

Channel model. The model of Nakagami-n (Rice) expresses the multipath channel that consists of one strong direct LOS signal and lots of random weaker signals. It can be either a Rayleigh or a Rician channel by adjusting the factor n. Below, (2) is the probability density function of the fading amplitude, ξ which is given as [9]

$$p_\xi(\xi;\omega,n)=\frac{2(1+n^2)^{-n^2\xi}}{\omega}\exp\left(-\frac{(1+n^2)\xi^2}{\omega}\right)\times I_0(2n\xi\sqrt{1+(n^2/\omega)}),$$

(2)

where n varies from 0 (Rayleigh) to ∞ (Rician). The mean of the squared fading amplitude $\overline{\xi^2}$ is denoted by ω. The zeroth-order modified Bessel function is denoted by $I_0(\cdot)$.

Receiver. Equation (3) is the received signal model [8].

$$r(t)=\sum_{k=1}^{K}s_k(t-\tau_k)$$
$$=\sum_{k=1}^{K}H_{0/1}a_k\alpha_k(\sigma_{tg})d_k(t-\tau_k)c_k(t-\tau_k)\cos(\omega_c t+\theta').$$

(3)

In (3), $H_{0/1}$ is 0 or 1 depending on the absence or presence of a target, respectively. The fading amplitude, denoted by a_k, has the same distribution as (2). The propagation delay of the kth signal traveling the distance R_t+R_r is denoted by k. The propagation delay–induced carrier shift is indicated by $\theta'=(-\omega_c t)$. The coefficient that accounts for the parameters of the bistatic radar equation, target RCS, and phase shift is α_k and is defined as follows:

$$\alpha_k(\sigma_{tg})=\sqrt{\frac{P_tG_tG_r\lambda^2\sigma_{tg}}{(4\pi^3(R_tR_r)^2}}\exp\left(-j\frac{2\pi(R_t+R_r)}{\lambda}\right),$$

(4)

where P_t and λ are the transmit power and wavelength, respectively. The transmitter and receiver gains are represented by G_t and G_r, respectively. The target RCS is represented by σ_{tg}. Under the noise-free condition, the jth signal in $r(t)$ can be recovered by multiplying the received signal with a time-synchronized replica of the jth signal, $c_j(t)$. That is,

$$r_j(t)=H_{0/1}a_j\alpha_j(\sigma_{tg})d_j(t-\tau_j)c_j(t-\tau_k)$$
$$\times\cos(\omega_c t+\theta')c_j(t-\tau')+\sum_{k=1(k\neq j)}^{K}\left(a_k\alpha_k(\sigma_{tg})\right.$$
$$\left.\times d_k(t-\tau_k)c_k(t-\tau_k)\cos(\omega_c t+\theta')c_j(t-\tau')\right),$$

(5)

where τ' is the estimated delay.

III. Proposed CRR Structure

In this section, we describe the functions of the CRR on a

module basis. The key concept of the CRR structure is the combination of the commercial rake receiver and the radar modules for target detection. The newly inserted radar modules M6–M12 (see Fig. 2) perform the signal processing for the threshold testing, demodulation, and detection. In M7 and M8, the DSF and SNR in the signals from intercepted paths are examined against the predefined threshold levels for M7 and M8, respectively. This two-step testing mechanism allows an adaptive detection depending on the validity of the radar measurements for a moving target under an FSF region. If a target echo appears at a certain finger, then detection is declared according to the decision rule in M7 or M8. Then, the signal of the specified finger is demodulated through M9 and M10 and compared for sameness against the reference signal. In the final stage, M11 computes the range and velocity of the target, based on the bistatic geometry information from M12. In implementing the CRR, simple hardware configurations, such as memory for data saving and information-transfer lines between modules, are inserted in a conventional rake receiver with minor modifications, and then radar modules can interact in parallel.

1. System Requirement Module (M6)

An operator sets up the system requirements, such as the detection probability (P_d), false alarm rate (P_{fa}), and the threshold of DSF (f_{th}), in the M6 module to determine the detection criteria in terms of SNR and DSF. The SNR threshold (ST), γ_{th}, is the criterion required to achieve a specified P_d and P_{fa} [10]. To get a value of ST, we employ the empirical model developed by Albersheim [11]. The criterion for f_{th}, is used to distinguish a fast moving target from other objects and can be set based on the DSF of the fastest one on the ground.

2. Rake Modules (M1–M5)

M1–M5 are the basic modules of a rake receiver (refer to Appendix). A coherent, fixed dwell parallel search scheme is adopted for time synchronization, which is a standard synchronization mechanism employed in rake [12]. First, we describe how a rake receiver receives a target echo in the time-domain (see Fig. 3). From the reference time, τ_{ref}, the multiple fingers L are arranged with equal time interval τ_{int}. Here, τ_{ref} is the round-trip time for a direct path. Scattered signals by a certain object will arrive at the receiver with a time delay and appear at a particular finger. It means that the reception time of the signal at each finger is corresponding to the range between a receiver and a target. In this manner, by flexibly adjusting τ_{int}, a rake receiver can receive a target echo returned within the maximum detection range. However, if a target is located in a range that is corresponding to the time between two
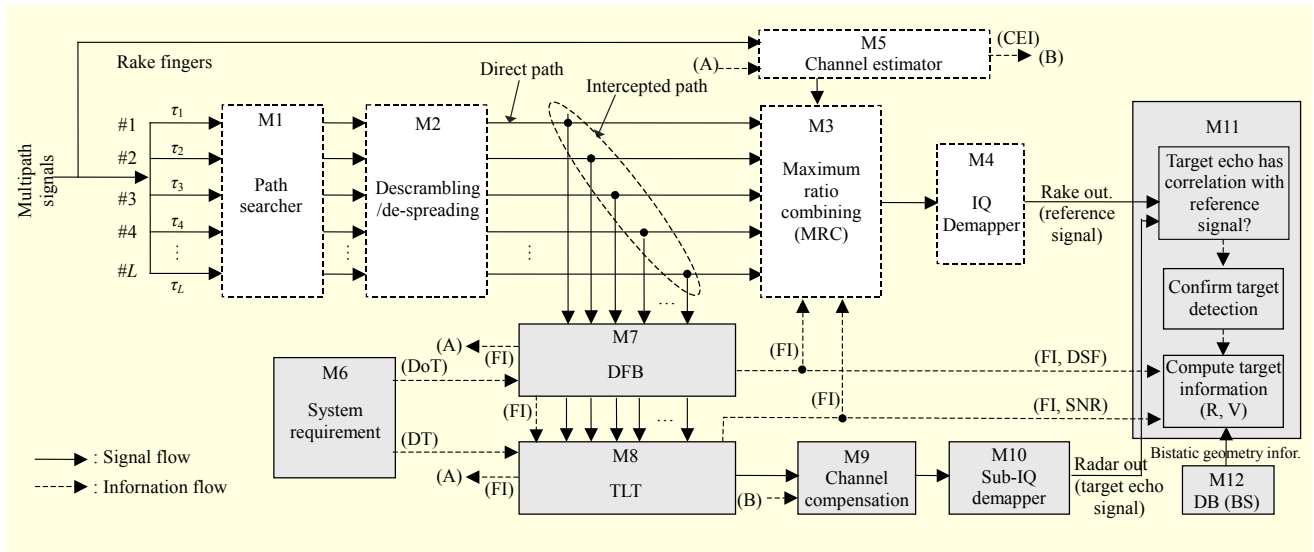
Fig. 2. Schematic diagram of proposed rake-based CRR: conventional rake modules (M1–M5) and newly inserted radar modules (M6 – M12).
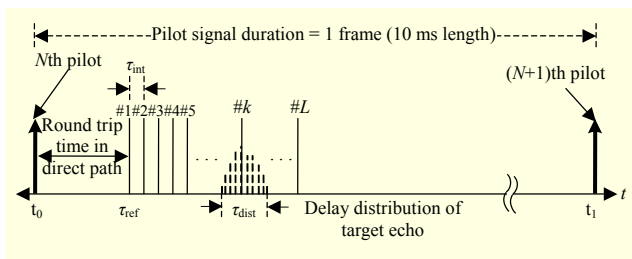

Fig. 3. Time-domain description for the reception of the target echo signals at the rake fingers.

Fig. 4. DFBs module.

consecutive fingers, a rake may miss a target echo. Therefore, a rake with densely arranged fingers is recommended. Since the target echo has a delay distribution due to multiple paths, one of the fingers can catch the signal in the case where $\tau_{int} < \tau_{dist}$ (Fig. 3). With L fingers, a receiver can cover the maximum detection range corresponding to the time $\tau_{ref} + L \cdot \tau_{int}$. Note that the target echo consists of a direct echo (reflected by only the target) and multipath echoes (reflected first by the target and then by other objects). However, in this paper we consider distributed target echo signals as one group because their separation is quite difficult.

Although the signals have been received, the receiver still does not know which finger holds the target echo signal. To get the finger index, we subsequently associate the rake module with DFB and TLT, which test the DSF and SNR level for each finger using the criterion of Doppler threshold (DoT) and ST, respectively.

3. DFB Module (M7)
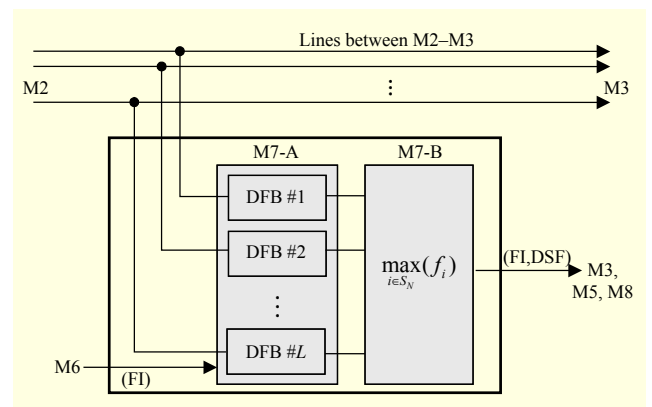
The DFB module (M7) plays a key role in determining the TD from the DSF associated with the rake module. Module M7 consists of two submodules, M7-A and M7-B, as shown in Fig. 4. It finds the finger index (FI) holding the target echo signal by testing the DoT for all the fingers. The signals passing through the direct path (between M2 and M3) are intercepted and then fed into the individually connected DFB, and then the cross-correlation process is performed with DSF replicas of the reference signal, which is locally generated using the PN sequence of the pilot signal, as shown Fig. 5. More specifically, each DFB in M7-A generates K reference signals within the range $-f_d$ to $+f_d$ with intervals of Δf. The received signal is cross-correlated to all reference signals. Then, the Doppler surface chart that quantifies the correlation value between a received signal and each reference signal in terms of DSF is generated [13]. If a target echo signal is present in the DFB of the ith finger, then f_i will exceed f_{th}; while, a DFB without a target echo generates nothing for radar measurement. For the
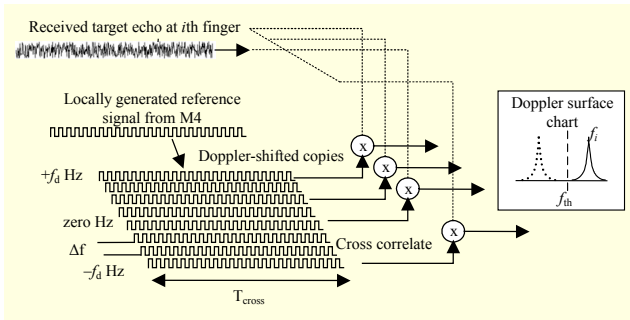
Fig. 5. Cross-correlation process of a DFB in M7-A (target echo signal and locally generated pilot sequence are correlated).

Fig. 6. Threshold level test module.

case when a DSF exceeding f_{th} appears in multiple DFBs, due to the delay distribution of target echoes, M7-B selects the finger index based on the criterion of (6),

$$i^* = \arg\max_{i \in S_N}(f_i),\qquad(6)$$

where $S_N = \{1, \dots, L\}$ is the set of the finger index. If the selected finger, f_{i*}, exceeds f_{th}, then M7-B regards the signal appearing at the ith finger as the echo from the target. Then, the information of i^* and f_{i*} is transferred to the connected M3, M5, and M8.

Sometimes, a moving target is located in the region of an FSF, where since the bistatic angle β_{bi} approaches 180°, the value of the DSF of the high-speed moving target becomes close to that of ground clutter [1]; therefore, we cannot determine TD based on DoT (that is, the DSF is no longer a detection criterion); so, a decision is handed over to the TLT, and M7-B subsequently informs nothing. As a countermeasure for this situation, ST testing is followed.

4. TLT Module (M8)

The TLT module (M8) consists of three submodules, as shown in Fig. 6. The role of this module is to test the ST condition for the finger specified by M7-B (that is, the i^*th finger). If M7-B informs nothing, then M8-A selects all the fingers (that is, set $S_S = S_N$). For both cases, M8-B tests whether the SNR at each finger exceeds the ST condition, as shown in Fig. 7. More specifically, each TLT compares the SNR at the finger with γ_{th} defined in M6. If a target echo exists in the jth finger, then γ_j will exceed γ_{th}. For the case that SNR exceeding γ_{th} appears in multiple TLTs due to the delay distribution of target echoes, M8-C selects the finger index with the strongest SNR based on the criterion of (7),

$$j^* = \arg\max_{j \in S_S}(\gamma_j),\qquad(7)$$

where j^* is the finger index holding the target echo signal. Once the process of M8 is complete, j^* and γ_j are informed to M3,
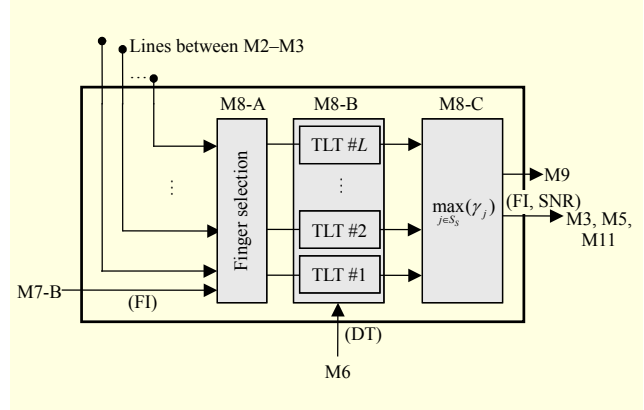
Table 1. Decision rule for target detection.

1st in DFB	2nd in TLT	Final decision
$f_{i*} > f_{th}$	Any	Detected at i^* (outside FSF)
$f_{i*} < f_{th}$	$\gamma_{j*} > \gamma_{th}$	Detected at j^* (inside FSF)
$f_{i*} < f_{th}$	$\gamma_{j*} < \gamma_{th}$	Not detected (any region)

M5, and M11.

Inside the FSF region, the strength of the received signal increases due to the effect of backward scattering; hence, here, a receiver is in a better position to target signal reception. In this situation, a pending decision for TD in a DFB is determined after the TLT process. Note that unlike the case of DSF, the SNR of the signal reflected by the objects on the ground may frequently exceed γ_{th} because of noise. Since it causes false alarm, our detection scheme considers DSF as a more decisive factor than SNR in target detection. The decision rule for TD is summarized in Table 1.

5. Demodulation Modules (M9–M10)

The target echo should be recovered to its original sequence to determine whether it is originated from a synchronized BS. For the i^* (or j^*)th finger, the target echo signal is demodulated through M9 and M10 and then compared with the reference signal in M11. Once the sameness of the two signals is verified, the TD is finally confirmed. A distorted phase rotation and attenuated amplitude of the i^* (or j^*)th finger's signal are compensated for using the channel estimation information (CEI) in M5.

6. TD Module (M11)

The TD module computes the range (R_r) and velocity (v_{tg}) of

a detected target based on information from DFB, TLT, and bistatic geometry. The finger index (i^* or j^*) from M7 or M8 indicates the time it takes for a pilot signal traveling from the transmitter to the receiver after reflection; that is, bistatic TOA.

$$R_t + R_r = \tau_{ref} + k\tau_{int} . \qquad (8)$$

In (8), k indicates the value of i^* or j^* and τ_{int} indicates a time interval between the fingers in Fig. 3. The distance $R_t + R_r$ can be transformed to R_r using the relationship between parameters on the bistatic plane, $R_r = \left[(R_t + R_r)^2 - BL^2 \right] / \left[2(R_t + R_r + BL\sin\theta_r) \right]$, where θ_r is the angle at the receiver to the target and BL is the base line in Fig. 1 [1]. If the transmitter and receiver are stationary, and the target is moving, then the target's bistatic DSF observed at the receiver site can be developed as [1]

$$f_{bi} = (2v_{tg} / \lambda) \cos\delta \, \cos(\beta_{bi} / 2) , \qquad (9)$$

where f_{bi} is f_{i^*}.

7. Data Base (M12)

The geometrical information and the positioning history of the detected target are stored in a data base (DB). To calculate BL, θ_r, β_{bi}, and δ in Fig. 1, we use the bistatic geometry information and a previously estimated target position. The receiver gets the distance BL using the original BS's location information. The latter is calculated and transmitted from M12 after completing a previous detection process and identifying the code sequence of the echo signal. As a result, θ_r, β_{bi}, and δ are computed by the geometrical construction based on the North-referenced coordination system.

IV. Evaluation of System Performance

The performance of the CRR is evaluated in terms of detection probability and maximum detection range. The system model is the same as in Fig. 1 and its parameters are depicted in Table 2.

1. Probability of Detection

We provide a definition of detection for the CRR. TD is achieved when the target echo signal not only satisfies the ST condition but also when its original sequence has been demodulated without bit error. According to the latter condition, the frame error rate (FER) for a pilot signal has to be considered in the calculation of the detection probability. For the ST condition, P_d is the system requirement being set in M6. To investigate the relationship between P_d, P_{fa}, and γ_{th}, we introduce the empirical model developed by Albersheim,

Table 2. System parameters.

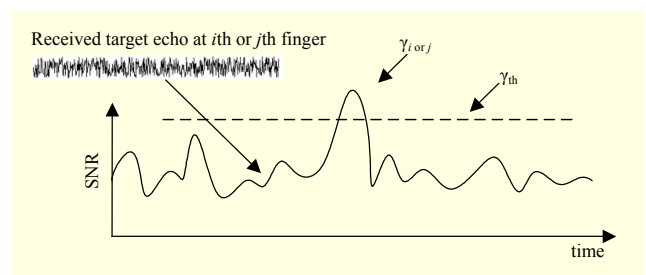| System bandwidth (B)	1.25 MHz
Carrier frequency (f_c)	800 MHz
Pilot power / length	12 W / 10 ms
Bits of a pilot (N^{bits})	1024
BS/CRR antenna gain (G_t/G_r)	18 / 0 dBi
Baseline (BL)	1 km
Target RCS (σ_{tg})	1 dB
False alarm (P_{fa})	$10^{(-3)}, 10^{(-5)}, 10^{(-7)}$
Averaged fading amplitude (ω)	1

Fig. 7. SNR threshold test of TLT in M8-B.

which is given as

$$\gamma_{th}^m = -5\log_{10}m + \left(6.2 + \frac{4.54}{\sqrt{m - 0.44}} \right)\log_{10}(\gamma_{th}^1) , \qquad (10)$$

where $\gamma_{th}^1 = A + 0.12AB + 1.7B$, $A = \ln[0.62/P_{fa}]$, and $B = \ln[P_d/(1 - P_d)]$. The subscript m is the number of independent pulses to be integrated. In this formula, FER is considered by replacing the P_d in (10) to $P_d(1 - P_{FER})$, where P_{FER} is an FER for the pilot signal and is given as $P_{FER} \le 1 - (1 - P_{b^F})^{Nbits}$ Nbits. The bit error rate (BER) in the fading channel is denoted by $P_{b^F} = Q\left(\sqrt{(2E_b/N_0)\alpha^2} \right)$. The fading amplitude is represented by α, and

$$Q(x) = \frac{1}{\sqrt{\pi}} \int_{1/\sqrt{2}}^{\infty} e^{-u^2} \, du.$$

Energy per bit and noise density are indicated by E_b and N_0, respectively [14].

Figure 8 shows P_d depends entirely on P_{fa} under the same channel condition. In this result, note that the effect of P_{FER} is negligible in the calculation of the detection probability because the pilot signal is designed to be demodulated successfully above 3 dB. Therefore, the use of the pilot signal as the radar signal is a very reasonable choice in terms of being able to satisfy the requirements of the calculation of the detection probability. Figure 9 shows the effect of a
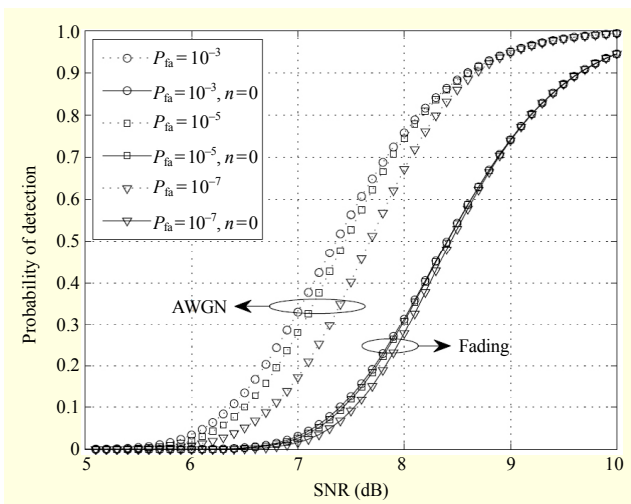
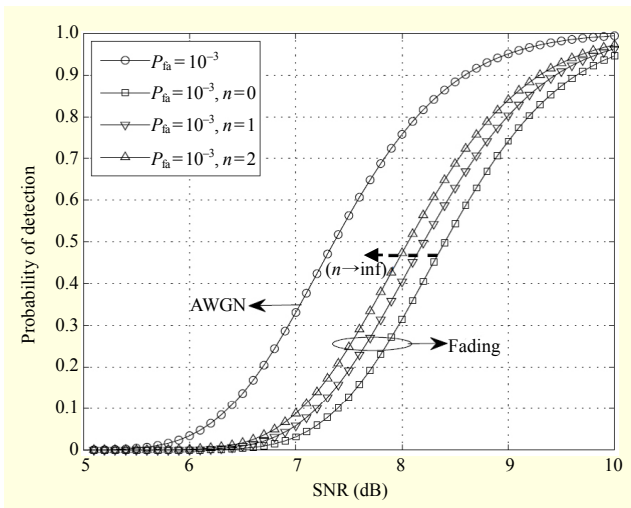Fig. 8. Detection probability vs. SNR, for variable P_{fa} and $n = 0$ or ∞.

Fig. 9. Detection probability vs. SNR, for variable Nakagami-n under the same $P_{fa} = 10^{-3}$.

Nakagami-n factor on P_d under the same P_{fa}. In our evaluation, we investigate the performance by varying n from 0 to 2. If the CRR located in the AWGN or multipath fading channel should satisfy $P_d = 0.9$, then the SNR of the ST condition becomes 8.5 dB or 9.4 dB, respectively. The result shows that in the multipath channel the CRR can guarantee the required detection probability by shifting the ST condition to the right by about 0.9 dB.

For the fading channel, the value of the SNR in the highest SNR region does not reach to 1, as shown in Figs. 8 and 9. The reason is that the pilot signal cannot be recovered completely under the severe fading channel condition (for small n), even if it is designed to be demodulated easily under a low SNR. In this case, according to the definition of detection, TD becomes failure.
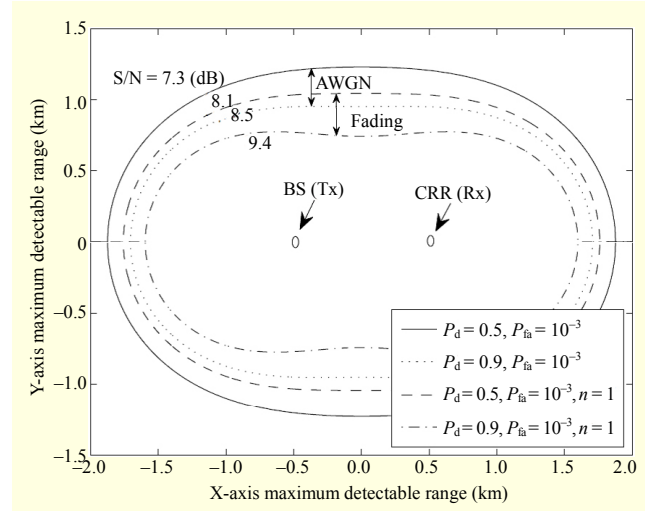

Fig. 10. Maximum detectable range ($R_t R_{r\,max}$) vs. minimum SNR (S_{min}).

2. Maximum Detection Range

The bistatic radar equation yields the minimum SNR (S_{min}) for the maximum detection range ($R_t R_{r\,max}$) where the required P_d and P_{fa} are satisfied. That is,

$$S_{min}(P_d, P_{fa}) = \frac{P_t \lambda^2 G_t G_r \sigma_{tg}}{(4\pi)^3 (R_t R_{r\,max})^2},\qquad(11)$$

where P_t, λ, $G_{t(r)}$, and σ_{tg} are depicted in (4). In Fig. 10, the range satisfying $P_d = 0.5$ to 0.9 and $P_{fa} = 10^{-3}$ is plotted by Oval of Cassini contour. For the requirement that $P_d = 0.9$ and $P_{fa} = 10^{-3}$, the CRR achieves $R_t R_{r\,max}$ at about 0.9 km to 1.3 km or 0.7 km to 1.1 km in AWGN or fading channel ($n = 1$), respectively.

V. Conclusion

In conclusion, we designed a new structure for the CRR using the concept of combining the rake receiver and the radar modules to detect a target located in a multipath channel. The proposed CRR has several advantages compared to its conventional counterpart. First, it easily achieves both the reception of a multipath signal and a time-synchronization by utilizing the basic functions provided by the rake receiver. Second, a fast moving target is adaptively detected depending on the validity of the DSF or SNR by the inserted radar modules. Finally, this structure can be implemented with only minor modifications to a rake receiver and the addition of simple hardware configurations. The results show that the CRR-utilizing pilot signal can guarantee a required detection performance and maximum detection range, even in the severe fading channel condition.

Appendix: Rake Receiver Operation and Time Synchronization

In Fig. 2, the path searcher (M1) allocates the number of fingers and the delay of each finger [15]. Its operational parameters are assigned by the finger management algorithm. The scrambling/spreading (M2) executes the inverse spreading of the received CDMA signal using the given code sequence to extract the desired signal. The same symbols obtained via different paths are then combined together, using the corresponding channel information, in a combining scheme such as maximum ratio combing (M3). The combined outputs are then sent to a simple decision device to decide on the transmitted bits (M4). In the channel estimator (M5), a distortion in the received signals is compensated by using CEI. Under a rake receiver, time synchronization with a desired original BS is achieved by the PN acquisition and tracking process. For the employed coherent fixed dwell parallel search synchronization scheme, the signal model and synchronization process are described in [12].

References

[1] N.J. Willis, *Bistatic Radar*, New York, USA: SciTech publishing, INC., 2005.

[2] Cellular Radar System. Accessed May 2011. http://www.roke.co.uk/skills/

[3] H. Sun, D.K.P. Tan, and Y. Lu, "Design and Implementation of an Experimental GSM Based Passive Radar," presented at the Proc. Int. Radar Conf., Adelaide, Australia, Sept. 3–5, 2003, pp. 418–422.

[4] H. Wang, J. Wang, and H. Li, "Target Detection Using CDMA Based Passive Bistatic Radar," *J. Syst. Eng. Electron.*, vol. 23, no. 6, Dec. 2012, pp. 858–865.

[5] P. Liu and J. Liu, "Analysis of Passive Targets Detection Using CDMA Signal," presented at the Proc. IEEE Int. Workshop VLSI Des. Video Techn., Shanghai, China, May 2005, pp. 408–410.

[6] S.K. Lee and H.C. Bang, *IMT-2000 CDMA technology,* Seoul, Rep. of Korea: Sehwa Pulishing, 2001.

[7] J.J. Caffery, *Wireless Location in CDMA Cellular Radio Systems*, 1st ed., Ohio, USA: Springer, 1999.

[8] L. Hanzo et al., *Single- and Multi-carrier DS-CDMA: Multi-user Detection, Space-Time Spreading, Synchronization, Networking, and Standards*, Chichester, England: IEEE Press, Wiley, 2003.

[9] M.S. Alouini and A.J. Goldsmith, "A Unified Approach for Calculating Error Rates of Linearly Modulated Signals over Generalized Fading Channels," *IEEE Trans. Commun.*, vol. 47, no. 9, Sept. 1999, pp. 1324–1334.

[10] D.A. Abraham, "Detection-Threshold Approximation for Non-Gaussian Backgrounds," *IEEE J. Oceanic Eng.*, vol. 35, no. 2, Apr. 2010. pp. 355–365.

[11] M. Skolnik, *Introduction to Radar System*, 3rd ed., New York, USA: McGraw Hill, 2001.

[12] H.G. Park, Y. Han, and M.J. Kim, *CDMA Communications*, The Institute of Electronics Engineers of Korea, Seoul, Rep. of Korea: Chungmun Publishing Company, 1998.

[13] P.E. Howland, D. Maksimiuk, and G. Reitsma, "FM Radio Based Bistatic Radar," *IEE Proc. Radar Sonar Navig.*, vol. 152, no. 3, June 2005, pp. 107–115.

[14] Contratto CSP-Omnitel per lo sviluppo di un simulatore per reti UMTS, Documento D00-B, "On SIR & BER Approximations in DS-CDMA System."

[15] A.J. Viterbi, *CDMA - Principles of Spread Spectrum Communication*, Massachusetts, USA: Addison Wesley, 1995.

Yeejung Kim received his MS and PhD degrees in electrical engineering from the Korea Advanced Institute of Science and Technology, Daejeon, Rep. of Korea, in 2007 and 2012, respectively. He is currently working as a senior engineer at the Smart-Car Research Institute of LG electronics, Seoul, Rep. of Korea. His research interests include LTE-A MAC protocol, cooperative relay networks, multi-static/MIMO radar system design, and radar signal processing algorithms. Recently, he has been working on the development of automotive radar systems and DSP algorithms.

Myungdeuk Jeong received his PhD degree in microwave engineering from Chungnam National University, Daejeon, Rep. of Korea, in 2003. He is currently a principal researcher at the Agency for Defense Development, Daejeon, Rep. of Korea, where he is involved in the development of radar systems. His research interests include microwave circuit design; radar transmitter and receivers; and phase array radar systems.

Youngnam Han received his BS and MS degrees in electrical engineering from Seoul National University, Seoul, Rep. of Korea, in 1978 and 1980, respectively. He received his PhD degree in electrical engineering from the University of Massachusetts, Amhest, USA, in 1992. He joined the Electronics and Telecommunications Research Institute, Daejeon, Rep. of Korea, in 1992, where he served as section head of the Mobile Telecommunications Division. From 1998 to 2009, he was a professor at the Information and Communications University, Daejeon, Rep. of Korea. Since 2009, he has been working as a professor at the Electrical Engineering Department, Korea Advanced Institute of Science and Technology, Daejeon, Rep. of Korea. His research interests include radio access specifications and performance evaluation in wireless communication systems. He is currently steering committee chair of the 5G Forum, Rep. of Korea.